Am J Physiol Renal Physiol 298: F335–F345, 2010.
First published November 25, 2009; doi:10.1152/ajprenal.00453.2009.

OCRL1 function in renal epithelial membrane traffic

Shanshan Cui,[1]* Christopher J. Guerriero,[1]* Christina M. Szalinski,[1] Carol L. Kinlough,[1] Rebecca P. Hughey,[1,2] and Ora A. Weisz[1,2]

[1]*Renal Electrolyte Division and* [2]*Department of Cell Biology and Physiology, University of Pittsburgh Medical School, Pittsburgh, Pennsylvania*

Submitted 5 August 2009; accepted in final form 23 November 2009

Cui S, Guerriero CJ, Szalinski CM, Kinlough CL, Hughey RP, Weisz OA. OCRL1 function in renal epithelial membrane traffic. *Am J Physiol Renal Physiol* 298: F335–F345, 2010. First published November 25, 2009; doi:10.1152/ajprenal.00453.2009.—The X-linked disorder Lowe syndrome arises from mutations in OCRL1, a lipid phosphatase that hydrolyzes phosphatidylinositol 4,5-bisphosphate (PIP_2). Most patients with Lowe syndrome develop proteinuria very early in life. PIP_2 dynamics are known to modulate numerous steps in membrane trafficking, and it has been proposed that OCRL1 activity regulates the biogenesis or trafficking of the multiligand receptor megalin. To examine this possibility, we investigated the effects of siRNA-mediated OCRL1 knockdown on biosynthetic and postendocytic membrane traffic in canine and human renal epithelial cells. Cells depleted of OCRL1 did not have significantly elevated levels of cellular PIP_2 but displayed an increase in actin comets, as previously observed in cultured cells derived from Lowe patients. Using assays to independently quantitate the endocytic trafficking of megalin and of megalin ligands, we could observe no defect in the trafficking or function of megalin upon OCRL1 knockdown. Moreover, apical delivery of a newly synthesized marker protein was unaffected. OCRL1 knockdown did result in a significant increase in secretion of the lysosomal hydrolase cathepsin D, consistent with a role for OCRL1 in membrane trafficking between the *trans*-Golgi network and endosomes. Together, our studies suggest that OCRL1 does not directly modulate endocytosis or postendocytic membrane traffic and that the renal manifestations observed in Lowe syndrome patients are downstream consequences of the loss of OCRL1 function.

proximal tubule; Lowe syndrome; phosphatidylinositol; megalin; CLC-5; endocytosis; cathepsin D

LOWE SYNDROME IS AN X-LINKED disorder characterized by congenital cataracts, mental retardation, and renal malfunction that results from mutations in the gene encoding oculocerebrorenal syndrome of Lowe (OCRL1) (7). OCRL1 is a lipid phosphatase that converts phosphatidylinositol 4,5-bisphosphate (PIP_2) to phosphatidylinositol 4-phosphate by hydrolyzing the 5′ phosphate of PIP_2 (44, 56). OCRL1 is localized primarily at the *trans*-Golgi network (TGN) and is also associated with a subset of endosomes and with clathrin-coated pits, suggesting a potential function of this enzyme in membrane traffic through these compartments (8, 9, 15, 16, 46). While mutations throughout the 970 amino acid protein encoded by the OCRL1 gene can result in Lowe syndrome, cell extracts from fibroblasts cultured from Lowe syndrome patients universally exhibit a markedly reduced ability to dephosphorylate PIP_2 (29, 44). OCRL1 appears to be the major PIP_2-hydrolyzing enzyme in human kidney proximal tubule cells, and kidney cells derived from Lowe syndrome patients have roughly double the normal cellular contingent of PIP_2 (55). Thus, the OCRL1 phenotype correlates well with loss of phosphatase activity.

Lowe syndrome patients almost universally have renal Fanconi syndrome, including acidosis, amino aciduria, phosphaturia, and proteinuria (7). The defect in protein reabsorption has been suggested to result from improper function or trafficking of the cell surface receptor megalin (30, 37). Megalin, a member of the LDL receptor family, is a 600-kDa transmembrane protein that recycles at the apical domain of polarized epithelial cells (10). Megalin binds to numerous protein ligands that dissociate from the receptor after internalization and are targeted to lysosomes for degradation. In patients with Fanconi syndrome, ligand handling is somehow compromised, resulting in excess secretion of filtered proteins into the urine. Whether proteinuria in Lowe syndrome patients is due to aberrant megalin trafficking as a result of the defect in OCRL1 activity has not been directly tested experimentally.

In addition to its role in signaling, PIP_2 also regulates cytoskeletal dynamics as well as numerous steps in membrane traffic (14, 50). We previously found that increases in cellular PIP_2 mediated by overexpression of phosphatidylinositol 4-phosphate 5-kinase type Iβ (PI5KIβ) in Madin-Darby canine kidney (MDCK) cells stimulated delivery kinetics of a subset of apical membrane proteins (18). Similarly, increased PIP_2 has been correlated with an increase in clathrin-mediated endocytosis (3, 39, 53).

Given the known stimulatory roles of PIP_2 in these processes, it is not immediately obvious how loss of OCRL1 function might lead to Fanconi syndrome in Lowe syndrome patients. Additionally, it is difficult to describe a mechanism leading to the ancillary renal defects that accompany proteinuria in Lowe syndrome patients, including acidosis, amino aciduria, and phosphaturia. Nevertheless, the idea that OCRL1 directly regulates megalin traffic has been reinforced by the recent demonstration that some patients with Dent disease, originally described as resulting from defective function of the CLC-5 Cl^-/H^+ antiporter, in fact have mutations in OCRL1 (24, 48). There is strong evidence that loss of CLC-5 function leads to decreased uptake of fluid phase markers and megalin ligands in knockout mouse models (11, 13, 19, 25, 43, 51, 52), although direct studies on megalin endocytosis have not been performed. The recent demonstration by De Camilli's group (16) that a small subpopulation of OCRL1 binds to APPL1 in clathrin-coated pits has fueled this speculation. OCRL1 also interacts with clathrin, α-adaptin, and several Rab proteins, including Rabs 5 and 6 (9, 12).

Although the OCRL1 protein is ubiquitously expressed in mouse and human tissues and cell lines, only a subset of organs are functionally impaired by OCRL1 mutations (38). It has been hypothesized that expression of other inositol polyphos-

* S. Cui and C. J. Guerriero contributed equally to this work.

Address for reprint requests and other correspondence: O. A. Weisz, Renal Electrolyte Div., 978.1 Scaife Hall, 3550 Terrace St., Pittsburgh, PA 15261 (e-mail: weisz@pitt.edu).

phatases can compensate for loss of OCRL1 function in some cells. Interestingly, knockout of the OCRL1 gene in mice does not recapitulate Lowe syndrome, as the mice do not develop cataracts or renal Fanconi syndrome (27). Expression of the homologous 75-kDa inositol polyphosphate-5-phosphatase INPP5B in mice has been suggested to compensate for loss of OCRL1 function, as INPP5B is expressed at considerably higher levels in mice compared with humans. In support of this idea, knockout of INPP5B in mice had no discernible renal phenotype; however, a cross between OCRL1 and INPP5B knockout mice did not produce any viable double-knockout mice (27). However, in contrast to OCRL1, INPP5B is largely localized to the early biosynthetic pathway, although it is also present on some early endocytic compartments. INPP5B does bind to APPL1 in vitro but unlike OCRL1, it does not interact with clathrin or α-adaptin (16, 54). Moreover, a recent study argues that OCRL1 and INPP5B do not access the same pools of PIP_2, as expression of INPP5B does not rescue membrane ruffling in OCRL1-deficient fibroblasts (12).

In the absence of an animal model, we used siRNA-mediated knockdown in human (HK-2) and canine (MDCK) renal epithelial cells to model the disease and examine the consequent effects on the trafficking of megalin and other proteins. MDCK cells establish well-differentiated monolayers and provide a good model in which to investigate apical biosynthetic and endocytic traffic; however, they also express significant levels of INPP5B, which could complicate dissection of the cellular role of OCRL1. The human proximal tubule cell line HK-2 is less well-differentiated but expresses no INPP5B. We find that knockdown of OCRL1 in either cell line recapitulates key features of cells cultured from Lowe Syndrome cells, including a trend toward increased cellular PIP_2 and alterations in cytoskeletal dynamics. We found no effect of depleting OCRL1 on either biosynthetic or endocytic membrane traffic. However, we did observe increased lysosomal hydrolase secretion in OCRL1-deficient cells, consistent with a role for this enzyme in post-Golgi delivery to lysosomes (8, 47).

MATERIALS AND METHODS

DNA constructs and adenoviruses. The megalin minireceptor consisting of the ligand binding domain 4, transmembrane domain, and cytoplasmic tail of megalin (M4 in Ref. 45) was kindly provided by Dr. M. Farquhar and modified by adding an extracellular V5 epitope tag and cytoplasmic GFP. The construct was subcloned into the pAdtet adenoviral expression vector and replication-deficient adenovirus (AV) was prepared. Generation of the AVs encoding OCRL1, PI5KIβ, influenza hemagglutinin (HA), and rabbit polymeric immunoglobulin receptor (pIgR) was described previously (18, 22). The mouse and human β and α isoform designations for PI5K are reversed. In this paper, we use the human isoform designation based on GenBank guidelines.

Cell culture and adenoviral infection. MDCK cells were cultured in MEM (Sigma) supplemented with 10% FBS, 100 U/ml penicillin, and 100 μg/ml streptomycin. Cells were plated on transwells (Costar) for 3–4 days before experiments. Human kidney proximal tubule HK-2 cells were obtained from ATCC and grown in DMEM-F12 medium (Sigma) supplemented with 5 μg/ml insulin, 0.02 μg/ml dexamethasone, 0.01 μg/ml selenium, 0.05 μg/ml transferrin, 2 mM L-glutamine, 10% FBS, 100 U/ml penicillin, and 100 μg/ml streptomycin. Adenoviral infection of MDCK-T23 cells and HK-2 cells was as described previously for cells growing on transwells or plastic dishes, respectively (21, 23). MDCK T23 cells stably maintain the tetracycline transactivator required for expression of most of our AV-encoded proteins. AV expressing this transactivator was included during infection of HK-2 cells.

Antibodies and indirect immunofluorescence. Affinity-purified monoclonal antibody directed against OCRL1 was the generous gift of Drs. R. Nussbaum and S. Suchy. Indirect immunofluorescence to detect endogenous OCRL1 was performed using a dilution of 1:100 primary antibody followed by Alexa488-conjugated secondary antibody (1:500; Invitrogen Molecular Probes). Cells were costained with polyclonal anti-furin antibody (1:200; Affinity Bioreagents) detected using Alexa647-conjugated goat anti-rabbit. Mouse anti-ARH and rabbit anti-Dab2 antibodies for Western blotting were generously provided by Dr. L. Traub. Surface megalin minireceptor was detected by incubation of cells on ice with mouse anti-V5 antibody (1:200; Invitrogen) and Alexa647-conjugated goat anti-mouse secondary antibody (1:500; Invitrogen Molecular probes) before fixation.

siRNA knockdown. All siRNA constructs were purchased from Dharmacon. A target sequence (GGTTCCCTGCCATTTTTCA) that efficiently knocks down OCRL1 was kindly provided by A. Ungewickell. There is an intentional single-nucleotide mismatch at the 3′ end of the sense sequence that enhances the efficiency of target mRNA degradation (17). This siRNA efficiently knocks down OCRL1 in both HK-2 and MDCK cells. SiRNA targeting canine N-WASP (GGCGAGACCCCCCAAATGC) was based on a published siRNA targeting rat N-WASP (28). SiRNA directed against firefly luciferase was used as a control. SiRNAs were introduced into MDCK and HK-2 cells using nucleofection as follows: cells cultured in growth media in 10-cm dishes were maintained so that a 50–60% density was achieved on the day of siRNA treatment. Cells were trypsinized from the dishes, counted using a hemocytometer, pelleted by centrifugation, and resuspended in Ingenio electroporation solution (Mirus; 4 million cells/100 μl solution). Suspended cells were mixed with control or OCRL1-specific siRNA (10 μg of siRNA per 4 million cells), transferred into Ingenio cuvettes (0.2-cm gap, Mirus; 100 μl cell suspension/cuvette), and electroporated in an Amaxa nucleofector (Lonza) using the program T20. After nucleofection, cells were immediately plated and cultured in growth media for 3 days before use. Knockdown of OCRL1 was confirmed for all experiments by Western blotting or by RT-PCR. Knockdown efficiency was typically >95% in MDCK cells and ~80% in HK-2 cells.

Determination of knockdown efficiency using RT-PCR. The Ambion RNAqueous phenol-free total RNA isolation kit was used to extract RNA from HK-2 and HeLa cell lysates, and RNA concentration was determined after DNase treatment using absorbance at 260 nm. Reactions containing 1 μg of RNA, 2 μl of Oligo(dT) primer (50 μM stock) and nuclease-free water in a total volume of 12 μl were mixed gently, spun briefly, heated for 3 min at 72°C, and set immediately on ice. Two microliters of 10× RT buffer, 4 μl dNTP mix, 1 μl of RNAse inhibitor, and 1 μl moloney murine leukemia virus reverse transcriptase (or water, for control samples) were added. The solution was then mixed gently and incubated at 42°C for 1 h, followed by incubation at 92°C for 10 min to inactivate the RT enzyme. A 3-μl aliquot of this reaction was mixed with 2.5 μl each sense and antisense primers (1 mg/ml), 5 μl of 10× PCR buffer, 0.5 μl of enzyme mix (GeneAmp High Fidelity PCR System, Applied Biosystems), 5 μl of DMSO, and 26.5 μl of PCR-grade water. The solution was pipetted into a 0.6-ml thin walled tube and placed into a Bio-Rad thermocycler. After a 1-min incubation at 95°C, the reaction was cycled 35 times at 95°C for 30 s, 52°C for 30 s, and 72°C for 30 s. Reactions were then incubated for a final 5 min at 72°C and held at 4°C. Five microliters of this reaction were loaded on a 2% agarose gel and product sizes were measured against a Track-It ladder (Invitrogen). The sense and anti-sense PCR primer sequences used were CAGATGTGAGCCACCACGC and GCGTGGTGGTTCATGCCTG for human INPP5B, GGAAGCCCTGCCAGAGCCTGT and ACGCTGACGGTCACTTGGAGT for canine INPP5B, and CACTGACCTGGGATCTTTG and CCAGCTGAATCCGAAATCC for human OCRL1. Actin primers

(ACCTTCAACTCCATCATGAAG and CTGCTGGAAGGTGGACAG for sense and anti-sense, respectively; which amplify both human and canine sequences) were included as positive controls in all experiments to confirm efficient RNA recovery.

Quantitation of actin comets. GFP-actin-expressing MDCK cells treated with OCRL1 or control siRNA were plated onto filters for 2 days before being transferred to Bioptech 0.17-mm ΔT dishes for an additional day before imaging using an Olympus IX-81 (Melville, NY) equipped with an UltraView spinning disc confocal head (PerkinElmer Life Sciences) and an argon-ion, argon-krypton, and helium-cadmium laser combiner. Three-minute movies were taken of random fields with either an Olympus ×60 PlanApo (NA 1.40) or a ×100 UPlanApo (NA 1.35) oil immersion objective. Movies were reviewed multiple times to determine the percentage of cells with actin comets.

Quantitation of PIP_2. MDCK cells treated with either control or OCRL1 siRNA were plated onto filters for 3 days. Phospholipids were labeled with ^{32}P-orthophosphate, extracted, and analyzed by thin-layer chromatography to determine relative phospholipids levels as described in Ref. 6.

Apical biosynthetic delivery kinetics of HA. MDCK cells (treated with control siRNA or siRNA directed against OCRL1 or N-WASP as noted) were seeded onto Transwell filters for 3 days. Cells were then infected with AV-HA, and where indicated, with control AV or AV-PI5KIβ. The following day, cells were starved in methionine-free medium, pulsed with [^{35}S]methionine (Easy Tag Express protein labeling mix; Perkin-Elmer), and chased for 2 h. Apical delivery was measured using a cell surface trypsinization assay as described in Ref. 22.

[^{125}I]lactoferrin binding to MDCK cells. Human lactoferrin (Sigma) was iodinated to a specific activity of 1,500–2,000 cpm/ng using the ICl method. Filter-grown MDCK cells were incubated for 1 h on ice with HEPES-buffered MEM containing [^{125}I]lactoferrin {[^{125}I]Lf; ~1,200,000 cpm/well}. For competition experiments, >100-fold surplus cold lactoferrin or BSA (negative control, Sigma) was included. After the incubation, cells were washed thoroughly with ice-cold medium, solubilized, and cell-associated radioactivity was quantitated using a γ-counter (Packard).

[^{125}I]Lf degradation and recycling in MDCK or HK-2 cells. Filter-grown MDCK cells (infected with AV-mini-megalin) or HK-2 cells on plastic were incubated on ice for 1 h with medium containing [^{125}I]Lf (~1,200,000 cpm/well; added apically to MDCK cells). Cells were washed thoroughly with ice-cold medium and then warmed up to 37°C to allow ligand uptake for various time periods. At each time point, the medium was collected. The cells were harvested after the final time point and solubilized. Tricholoroacetic acid (TCA) was added to the medium at a final concentration of 10% and the samples were incubated for 20 min on ice. After centrifugation, TCA-soluble and -insoluble ^{125}I was quantitated using a γ-counter, and degraded/recycled lactoferrin was determined (TCA-soluble/insoluble ^{125}I cpm divided by the total ^{125}I cpm recovered in the cells and medium).

[^{125}I]Lf degradation in HK-2 cells. Nonpolarized HK-2 cells treated with control or OCRL1 siRNA were incubated in GIBCO Opti-MEM I reduced serum medium (Invitrogen) containing [^{125}I]Lf (~200,000 cpm/well) in a 37°C incubator overnight (14–18 h). Blank wells containing [^{125}I]Lf in medium (no cells) were incubated under the same conditions to determine nonspecific [^{125}I]Lf degradation (background). After the incubation, the medium was collected and TCA was precipitated as described above. Cells were solubilized and subjected to the Dc protein assay (Bio-Rad). The amount of [^{125}I]Lf degraded in each sample was calculated as TCA-soluble counts above background normalized to total protein levels.

Endocytosis of mini-megalin. Endocytosis of mini-megalin was assessed using a biotinylation-based assay performed using the protocol previously described for MUC1 (2). Briefly, HK-2 cells infected with AV-mini-megalin (and either coinfected with AV-PI5KIβ or control AV, or treated with OCRL1 or control siRNA) were biotinylated on ice using sulfo-NHS-SS-biotin (Pierce). Cells were then rapidly warmed to 37°C for 0 or 6 min (one of the experiments comparing control and PI5KIβ AVs was warmed for only 5 min). Biotin on the cell surface was stripped with 2-mercaptoethane sulfonate (MESNa) before cells were solubilized in a HEPES-buffered detergent solution (60 mM octyl-β-D-glucopyranoside, 50 mM NaCl, 10 mM HEPES, 0.1% SDS, pH 7.4). Duplicate 0′ samples were left unstripped to quantitate total biotinylated mini-megalin at the cell surface. Biotinylated proteins were recovered after immunoprecipitation with avidin-conjugated beads and analyzed by Western blotting (to detect the V5 tag on mini-megalin) after SDS-PAGE. The percentage of mini-megalin endocytosis at each time point was calculated as the percent of total biotinylated signal remaining at 6 min minus the percent remaining at 0′ (background).

Endocytosis of [^{125}I]IgA. Iodination of IgA was performed essentially as described in Ref. 5. HK-2 cells nucleofected with control or OCRL1 siRNA were plated in 12-well dishes and infected with AV-pIgR after 2 days. The following day, cells were incubated with [^{125}I]IgA for 1 h on ice and then washed extensively with ice-cold medium to remove unbound radioligand. The cells were then incubated in prewarmed medium in a 37°C waterbath for 0, 2.5, or 5 min and then rapidly chilled. To remove [^{125}I]IgA from the cell surface, cells were incubated for 30 min on ice with 100 μg/ml L-1-tosylamide-2-phenylethylchloromethyl-ketone-treated trypsin (Sigma) and then stripped with 150 mM glycine buffer, pH 2.3, for 15 min on ice. Finally, cells were solubilized in 50 mM Tris · HCl, 2% Nonidet *P*-40, 0.4% deoxycholate, 62.5 mM EDTA, pH 7.4, and cell-associated radioactivity was determined using a gamma counter. Internalized [^{125}I]IgA was quantitated relative to total [^{125}I]IgA (recovered in the cells, trypsin and glycine strips, and the medium).

Quantitation of cathepsin D secretion. HK-2 cells were cultured for 3 days after nucleofection with either control or OCRL1 siRNA. Cells were then pulse labeled with [^{35}S]methionine and chased for 4 h. NH_4Cl (10 mM) was included in some samples as a positive control. Following the chase, both the cells and the media were harvested and immunoprecipitated using an anti-cathepsin D antibody (Upstate). Radioactive cathepsin D secreted into the medium during the chase was quantitated following separation by SDS-PAGE.

RESULTS

Characterization of OCRL1 knockdown in human and canine kidney cells. To examine the consequences of disrupting OCRL1 function in renal epithelial cells, we optimized approaches to knockdown the protein using siRNA. We previously showed that biosynthetic delivery in polarized MDCK cells is sensitive to overexpression of wild-type OCRL1 (18). However, because canine cells, like mice, might express a redundant inositol polyphosphate 5′-phosphatase that could compensate for loss of OCRL1, we also developed methods to knockdown OCRL1 in human renal proximal tubule HK-2 cells. Endogenous OCRL1 localized largely to the Golgi complex in both of these cell lines (Fig. 1*A* and data not shown). Other groups previously reported that a small subpopulation of OCRL1 also localizes to endosomes and the cell surface (8, 16, 46). Introduction of siRNA oligonucleotides by electroporation resulted in efficient reduction in OCRL1 levels in both cell lines, as measured by Western blotting (Fig. 1*B*) or using a PCR-based assay (performed using HK-2 cells only; Fig. 1*C*). Importantly, we could detect no endogenous expression of INPP5B message in either HK-2 or HeLa cells, although our primers efficiently amplified a heterologously expressed human INPP5B cDNA construct when expressed in HeLa cells (Fig. 1*D*). Thus, any functions of OCRL1 that are disrupted upon knockdown of this enzyme are unlikely to be restored by

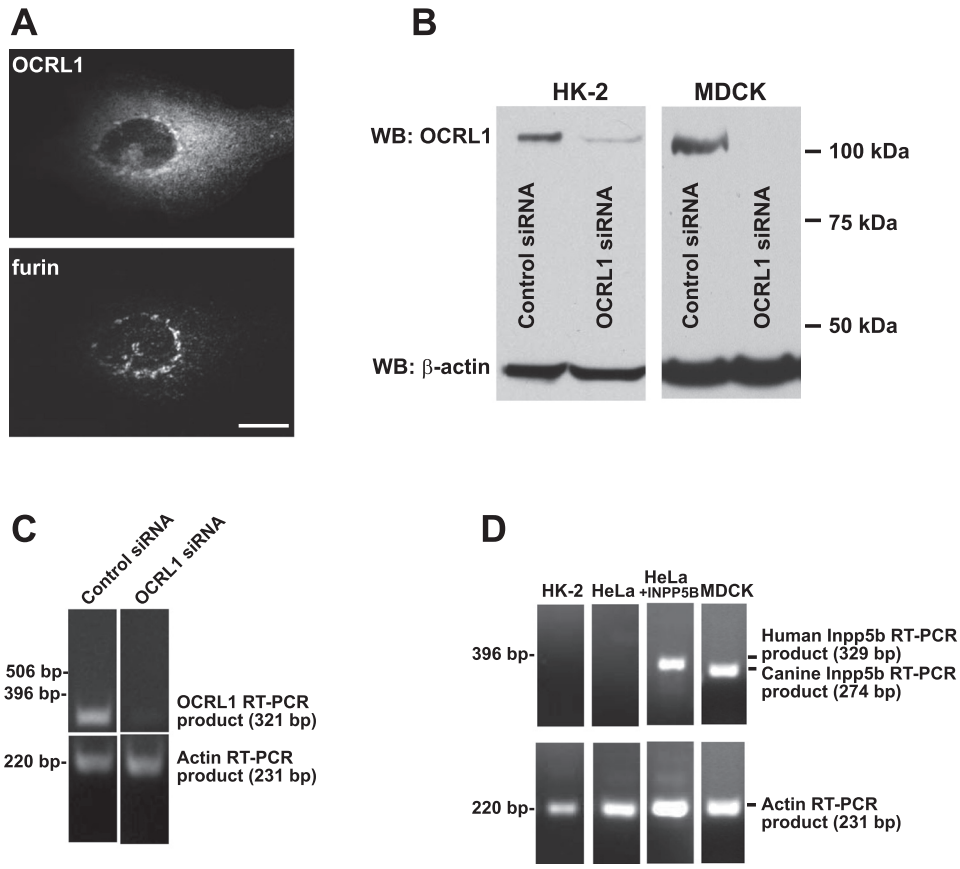

Fig. 1. siRNA-mediated knockdown of oculocerebrorenal syndrome of Lowe (OCRL1) in human and canine cells. *A*: Madin-Darby canine kidney (MDCK) cells were fixed, processed for indirect immunofluorescence to detect OCRL1 and the *trans*-Golgi network (TGN) marker furin, and examined using confocal microscopy. The images are maximum projections of 10 confocal slices. Scale bar: 10 μm. *B*: low-passage MDCK or HK-2 cells were nucleofected with control or OCRL1 siRNA as described in MATERIALS AND METHODS. Cells were plated directly onto permeable supports (MDCK) or in 12-well dishes (HK-2) for 3 days. Samples were harvested and analyzed by Western blotting (WB) to detect OCRL1 and actin (as a loading control). The migration of molecular mass standards is indicated on the *right*. *C*: siRNA knockdown of OCRL1 in HK-2 cells was confirmed using a PCR-based assay as described in MATERIALS AND METHODS. *D*: primers specific for human INPP5B were used to amplify mRNA isolated from HK-2 or HeLa cells. HeLa cells transfected with a cDNA encoding human INPP5B were included as a positive control to demonstrate the efficacy of the primers.

compensatory expression of INPP5B in these cells. However, MDCK cells do express significant levels of INPP5B (Fig. 1*D*).

Kidney proximal tubule cell lines derived from Lowe syndrome patients have been reported to have elevated levels of PIP_2 compared with normal human kidney cells (55); however, no other studies reported changes in cellular PIP_2 in OCRL1-deficient cells. This is consistent with the fact that most of the cellular PIP_2 is present at the plasma membrane, whereas OCRL1 is largely excluded from this site. We compared cellular PIP_2 extracted from control and OCRL1 knockdown cells after radiolabeling with $^{32}P_i$ for 4 h. We reproducibly observed a tendency toward increased cellular PIP_2 in MDCK cells treated with siRNA directed against OCRL1, although this was not statistically significant by Student's paired *t*-test (Fig. 2*A*). To determine whether this trend is physiologically relevant, we tested whether knockdown of OCRL1 alters the percentage of cells producing actin comets. Fibroblasts from Lowe patients have previously been demonstrated to have dramatically increased numbers of comets, presumably due to enhanced PIP_2-dependent activation of N-WASP-Arp2/3-mediated polymerization of these branched actin structures (1). To quantitate actin comet occurrence, control vs. OCRL1 knockdown MDCK cells stably expressing GFP-actin were observed by spinning disc confocal microscopy. Individual fields were imaged over a 3-min period and the number of cells with actin comets was quantitated. Knockdown of OCRL1 resulted in a dramatic increase in the percentage of cells with detectable actin comets over this period, confirming that OCRL1 normally regulates a pool of PIP_2 involved in cytoskeletal dynamics in these cells (Fig. 2*B*). Moreover, this pool is apparently not accessible to the INPP5B expressed in MDCKs. This is consistent with recent results demonstrating that expression of INPP5B does not rescue the enhanced membrane ruffling observed in OCRL1-deficient fibroblasts (12).

Effects of OCRL1 knockdown on biosynthetic delivery kinetics. We showed previously that elevation of cellular PIP_2 upon overexpression of PI5KIβ in polarized MDCK cells stimulates a post-Golgi step in biosynthetic delivery of the apical marker influenza HA via a mechanism dependent on actin comets (18). In contrast, heterologous expression of OCRL1 or dominant negative inhibitors of Arp2/3 activation inhibited HA delivery. Moreover, HA could be detected at the tips of actin comet-like structures in fixed cells. Because both PI5KIβ overexpression and OCRL1 knockdown cause an increase in actin comets, we hypothesized that HA delivery kinetics might be stimulated upon depletion of OCRL1 by siRNA. However, we found no effect of OCRL1 knockdown on HA delivery kinetics in either MDCK or HK-2 cells (Fig. 3, *A* and *B*). In contrast, knockdown of N-WASP resulted in significant inhibition of HA delivery in MDCK cells, whereas overexpression of PI5KIβ stimulated HA delivery kinetics as expected (Fig. 3*A*). PI5KIβ overexpression has a greater effect on cellular PIP_2 levels compared with OCRL1 knockdown [210% of control for PI5KIβ (C. J. Guerriero, unpublished results)], and it is possible that a threshold increase in PIP_2 is required to stimulate HA delivery.

Effect of OCRL1 knockdown on low-molecular-weight protein uptake and megalin internalization kinetics. We next examined whether knockdown of OCRL1 disrupts megalin-dependent uptake of low-molecular-weight proteins (LMWPs).

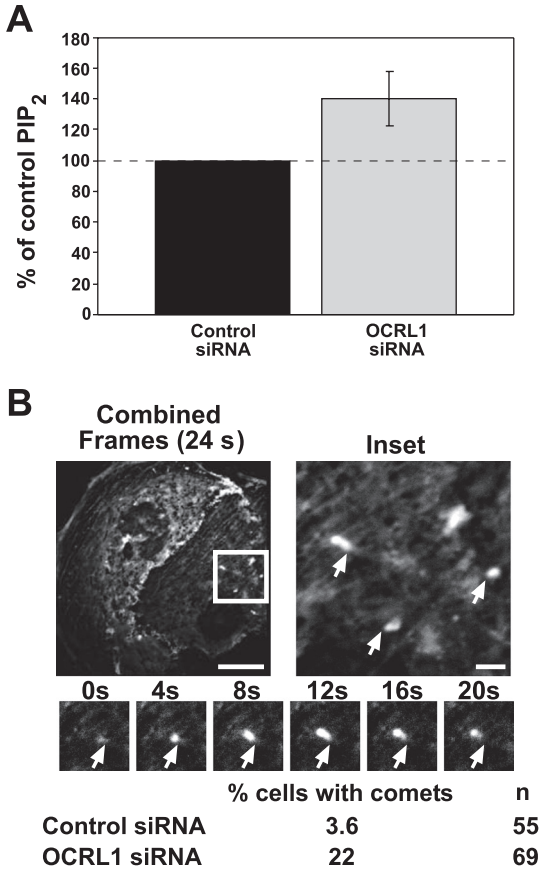

Fig. 2. Phosphatidylinositol 4,5-bisphosphate (PIP_2) levels and actin comet frequency are elevated upon OCRL1 knockdown in MDCK cells. *A*: MDCK cells were treated with either control or OCRL1 siRNA and plated directly onto filters for 3 days. Phospholipids were labeled with [^{32}P]orthophosphate and analyzed by TLC to determine relative phospholipids levels as described in MATERIALS AND METHODS. PIP_2 values in cells nucleofected with OCRL1 siRNA were normalized to control in 3 independent experiments and means ± SE are plotted. The difference in PIP_2 levels between the 2 experimental conditions is not statistically significant by Student's *t*-test. *B*: MDCK cells stably expressing GFP-actin were electroporated with control or OCRL1 siRNA and plated onto filters for 2 days before being transferred to Bioptech 0.17-mm ΔT dishes for an additional day before imaging. Images were taken every 2 s. MetaMorph software was used to overlay multiple frames and filter out low-level fluorescence to reveal the path of the actin comets in the cell (*right*; arrows). *Bottom*: path of a single comet. In each image, the arrow represents the starting position of the actin comet in the series. The percentage of cells treated with control vs. OCRL1 siRNA that had detectable actin comets during a 3-min imaging window is noted underneath; *n* represents the number of cells examined for each condition. Scale bar: 10 μm.

Patients with Dent disease caused by defective CLC-5 activity have virtually identical urinary proteomes to OCRL1 patients, and dramatically decreased uptake of megalin ligands has been observed in proximal tubule cultures from CLC-5 knockout mice (11). Moreover, megalin expression is reduced in proximal tubules from CLC-5 knockout mice (11) as well as in the renal tubular epithelium of some Dent disease patients (42). However, whether loss of CLC-5 function affects the kinetics or fidelity of megalin trafficking is unknown.

MDCK cells do not express endogenous megalin (45), although they do express LRP, a basolaterally recycling member of the LDL receptor family closely related to megalin. Additionally, these cells express both ARH and Dab-2, adaptor proteins thought to play a role in endocytosis of megalin in the proximal tubule. HK-2 cells express ARH, but not Dab-2 (Fig. 4*A*). The ARH doublet observed in MDCK cells has been previously observed in some other cell types (35). We infected polarized MDCK cells with recombinant AV expressing a GFP- and V5-tagged truncated megalin receptor (AV-mini-megalin). Fluorescence imaging in nonpermeabilized cells to selectively label the surface-exposed V5 tag in addition to the total pool of GFP-tagged mini-megalin confirmed that this protein was efficiently trafficked to the apical membrane (Fig. 4*B*). We next examined the domain-selective binding of [^{125}I]Lf, a ligand that binds to mini-megalin, in control vs. mini-megalin expressing MDCK cells. MDCK cells grown on Transwell filters were incubated with apically or basolaterally added ligand on ice and then quickly washed several times with ice-cold medium. The filters were removed from their supports and cell surface radioactivity was quantitated using a gamma counter. Apical binding to cells infected with AV-mini-megalin was significantly higher than control

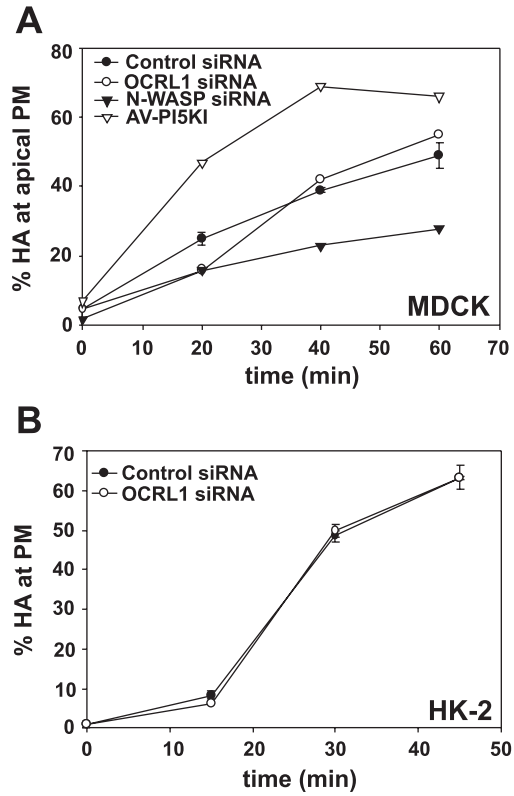

Fig. 3. Knockdown of OCRL1 does not enhance apical biosynthetic delivery kinetics in MDCK, HK-2 cells. *A*: MDCK cells were electroporated in buffer containing either control siRNA or an siRNA oligonucleotide directed against N-WASP or OCRL1. The efficiency of N-WASP knockdown was between 15 and 40% based on WB of cell lysates (not shown). The cells were seeded onto Transwell filters for 3 days and then infected with adenovirus (AV) expressing the apical protein hemagglutinin (HA) and either control AV or AV-PI5KIβ. The following day, cells were starved, radiolabeled for 15 min, and chased for 2 h at 19°C. Cell surface delivery kinetics of HA were measured after warming to 37°C using a cell surface trypsinization assay. Similar results were obtained in 3 independent experiments; results from a single representative experiment are plotted. *B*: HK-2 cells treated with either control or OCRL1 siRNA were infected with AV-HA 2 days after nucleofection. The following day, cells were radiolabeled for 15 min and plasma membrane delivery kinetics of HA were quantitated. Similar results were obtained in 4 independent experiments; results from a single representative experiment are plotted.

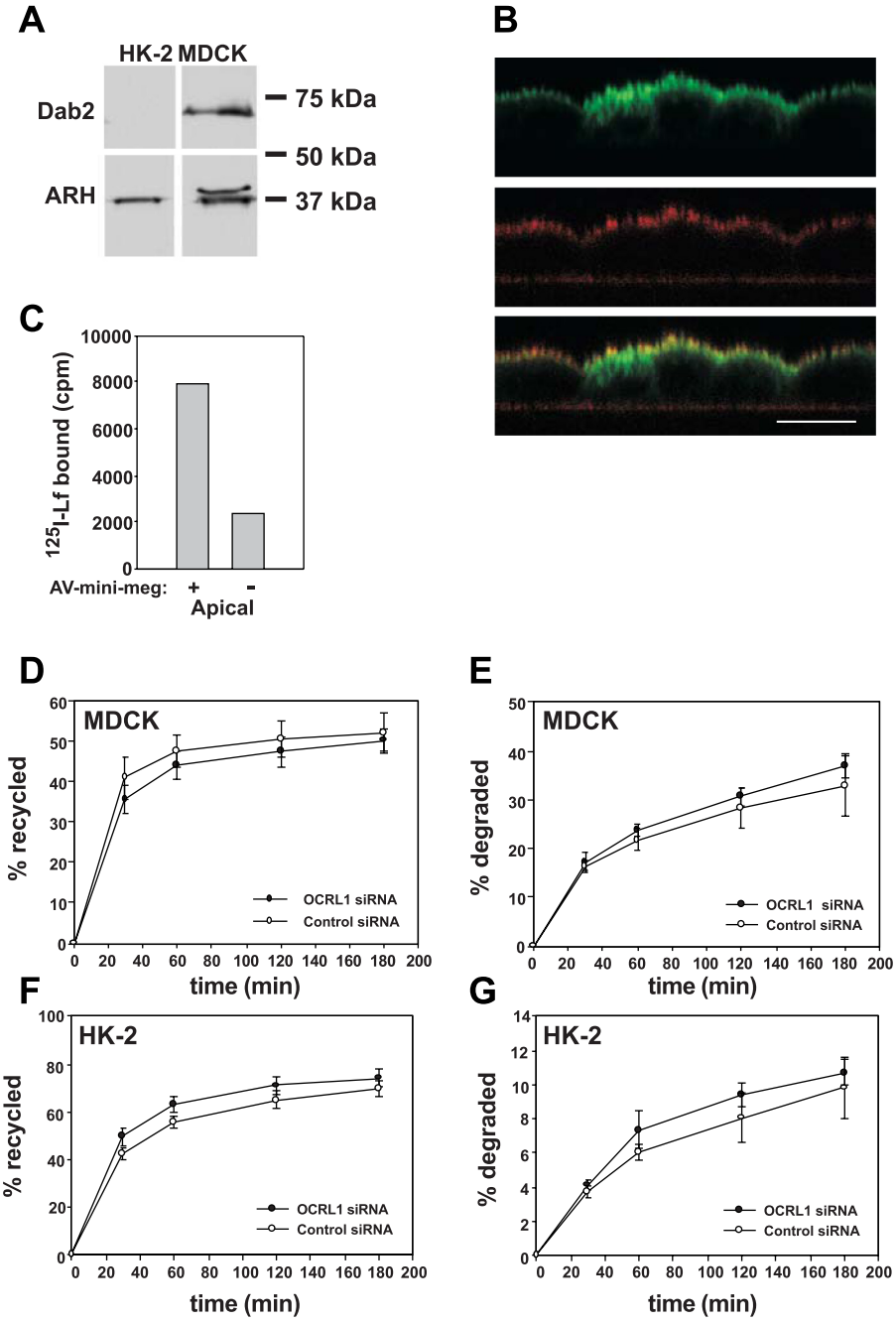

Fig. 4. OCRL1 knockdown does not affect megalin-mediated uptake and degradation of lactoferrin (Lf) in MDCK and HK-2 cells. *A*: comparable levels of MDCK and HK-2 cell lysates were blotted with antibodies against ARH and Dab-2. The migration of molecular mass standards is indicated on the *right*. *B*: filter-grown MDCK cells were infected with replication-defective recombinant AV encoding V5- and GFP-tagged mini-megalin. Cells were incubated on ice with anti-V5 antibody and secondary antibody to label the surface population of mini-megalin (red) and then fixed and processed for confocal microscopy. The total cellular population of mini-megalin was visualized using the GFP label (green). Scale bar: 10 μm. *C*: filter-grown MDCK cells infected with control AV or AV encoding mini-megalin were incubated with apically added [^{125}I]Lf on ice, then washed, solubilized, and cell-associated radioactivity was quantitated using a gamma counter. MDCK (*D*, *E*) or HK-2 (*F*, *G*) cells treated with control or OCRL1 siRNA were incubated with [^{125}I]Lf as described in MATERIALS AND METHODS. MDCK cells were infected with AV-mini-megalin 1 day before the experiment. The kinetics of Lf recycling (*D*, *F*) and degradation (*E*, *G*) were quantitated. Similar results were obtained in 3 independent experiments for each cell type.

cells, confirming that apical [^{125}I]Lf binding is quantitatively mediated by mini-megalin (Fig. 4*C*).

We then monitored the postendocytic fate of [^{125}I]Lf internalized apically from control and OCRL1 knockdown MDCK cells infected with AV-mini-megalin. As shown in Fig. 4, *D* and *E*, we observed no difference in the kinetics of recycling or degradation of this ligand in cells lacking OCRL1 compared with control cells. Moreover, OCRL1 knockdown had no effect on the kinetics of [^{125}I]Lf recycling or degradation mediated by endogenous megalin in HK-2 cells (Fig. 4, *F* and *G*).

Because the effect of OCRL1 on megalin-mediated handling of [^{125}I]Lf could be too subtle to detect in a single round of endocytosis, we also examined cumulative degradation of ligand over a prolonged incubation period (Table 1). HK-2 cells nucleofected with control or OCRL1 siRNA were incubated overnight with [^{125}I]Lf and release of TCA-soluble counts was quantitated. No effect of OCRL1 knockdown on the amount of [^{125}I]Lf degraded was observed using this integrated approach. Together, our studies suggest that uptake and degradation of megalin ligands are unaffected by loss of OCRL1 function in human and canine kidney cells.

A recent study found a small pool of OCRL1 associated with the adaptor APPL1 in clathrin-coated pits (16). Because APPL1 also associates through megalin via the adaptor GIPC, it was suggested that OCRL1 may play a role in endocytosis of a megalin-containing complex. We therefore directly examined the effect of OCRL1 knockdown on the initial rate of megalin internalization using a biotinylation/stripping approach. HK-2

Table 1. *OCRL1 knockdown in HK-2 cells does not affect lactoferrin degradation*

	Control siRNA, cpm	OCRL1 siRNA, cpm	OCRL1 KD/Control
Exp. 1	44,137 ± 4,035	35,952 ± 9,995	0.81
Exp. 2	31,216 ± 8,761	40,648 ± 5,172	1.30
Exp. 3	5,246 ± 2,261	4,747 ± 1,704	0.91
Exp. 4	3,085 ± 116	4,577 ± 1,259	1.48
Average	N/A	N/A	1.13 ± 0.32

Values are means ± SE. HK-2 cells treated with control or OCRL1 siRNA were incubated overnight with ^{125}I-Lf and TCA-soluble counts were recovered to quantitate cumulative ^{125}I-Lf degradation. Results from 4 independent experiments are shown. *Experiments 1* and *2* were performed using a different batch of ^{125}I-Lf compared with *3* and *4*.

cells treated with control or OCRL1 siRNA and infected with AV-mini-megalin were biotinylated using sulfo-NHS-SS-biotin on ice and then warmed to 37°C for 0 or 6 min. At each time point, samples were rapidly chilled, and remaining surface biotin was stripped with the membrane-impermeant reducing agent MESNa. Duplicate biotinylated samples were not warmed and left unstripped to measure the total amount of biotinylated megalin at the start of the time course. Cells were solubilized and biotinylated megalin was recovered and analyzed by Western blotting. As a control, we also examined the effect of PI5KIβ overexpression on megalin endocytosis kinetics. We previously demonstrated that overexpression of this enzyme stimulates endocytosis of other apical proteins, presumably by increasing surface levels of PIP_2 (53). As shown in Fig. 5*A*, knockdown of OCRL1 had no effect on megalin internalization. In contrast, megalin endocytosis was enhanced upon overexpression of PI5KIβ. Moreover, OCRL1 knockdown had no effect on the internalization kinetics of [^{125}I]IgA internalization mediated by a different surface receptor (the pIgR) expressed using AV in either HK-2 (Fig. 5*B*) or MDCK cells (C. M. Szalinski, unpublished results). Like megalin, pIgR endocytosis is clathrin-mediated, but pIgR does not contain ARH/Dab-2 binding motifs. Together, these data suggest that OCRL1 is not directly involved in internalization or postendocytic trafficking of megalin and its ligands, or of other membrane receptors.

Lysosomal hydrolase delivery in OCRL1 knockdown cells. Previous studies demonstrated that OCRL1 knockdown in HeLa cells resulted in partial redistribution of the cation-independent mannose 6-phosphate receptor from the TGN to endosomal structures. Moreover, OCRL1 patients are reported to have increased levels of lysosomal hydrolases in their serum (47). To determine whether depletion of OCRL1 affects delivery of lysosomal hydrolases in renal epithelial cells, we quantitated cathepsin D secretion in HK-2 cells treated with control or OCRL1 siRNA. Cells were radiolabeled for 2 h and returned to culture in serum-free medium. Media were collected after a 4-h chase and released cathepsin D, recovered after immunoprecipitation and SDS-PAGE, was quantitated using a phosphorimager. As shown in Fig. 6, knockdown of OCRL1 in HK-2 cells consistently resulted in a roughly 20% increase in cathepsin D secretion. This increase is comparable to that observed on incubation of HK-2 cells with ammonium chloride, which inhibits lysosomal delivery of newly synthesized soluble hydrolases (Fig. 6).

DISCUSSION

We optimized conditions to efficiently knockdown OCRL1 in both human (HK-2) and canine (MDCK) renal epithelial cells and measured the consequences on cellular PIP_2, actin comet frequency, and biosynthetic and postendocytic delivery. Depletion of OCRL1 did not have a significant effect on cellular PIP_2 levels but increased actin comet formation. However, we did not detect any effects of OCRL1 knockdown on the kinetics of apical biosynthetic delivery of HA or on megalin endocytosis, two trafficking steps that are stimulated when cellular PIP_2 is increased by overexpression of PI5KIβ. In contrast, we observed a significant increase in the secretion of the lysosomal enzyme cathepsin D in cells lacking OCRL1, consistent with previous observations that plasma lysosomal

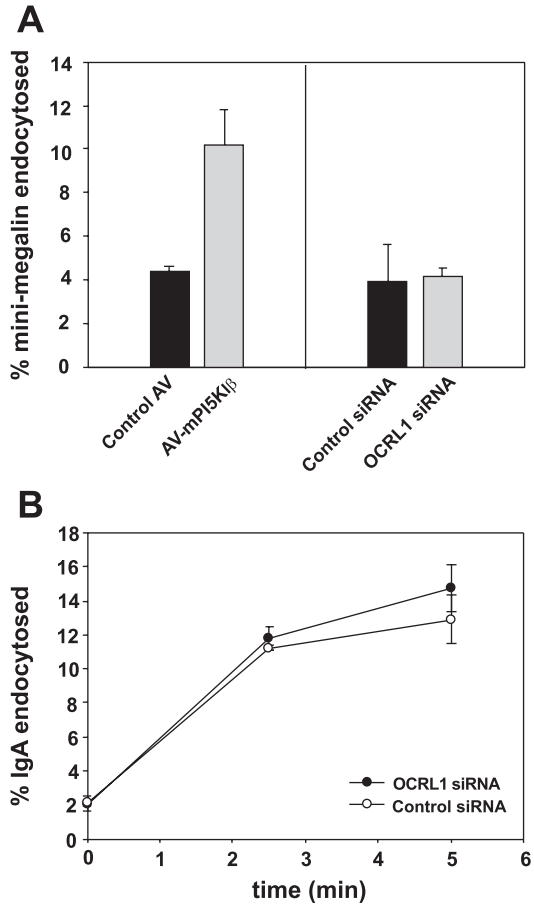

Fig. 5. OCRL1 knockdown does not affect endocytosis of megalin in HK-2 cells. *A*: effect of PI5KIβ overexpression (*left*) or OCRL1 knockdown (*right*) on endocytosis of mini-megalin was quantitated using the biotinylation-based assay described in MATERIALS AND METHODS. HK-2 cells treated with control or OCRL1 siRNA or infected with control or PI5KIβ expressing AVs as indicated were biotinylated on ice and then warmed to 37°C for 0 or 6 min. Samples were stripped to remove surface biotin and endocytosis was quantitated by WB after recovery of residual biotinylated mini-megalin. One set of 0-min samples was left unstripped so that results could be normalized to total mini-megalin at the surface before warming up. The mean endocytosis (±SE) from 3 experiments comparing PI5KIβ overexpression to control AV and 4 experiments comparing OCRL1 and control siRNA are plotted. *B*: endocytosis of [^{125}I]IgA by polymeric immunoglobulin receptor (pIgR)-expressing HK-2 cells nucleofected with either control or OCRL1 siRNA was performed as described in MATERIALS AND METHODS. The means ± range of duplicate samples is shown. Similar results were obtained in 2 experiments.

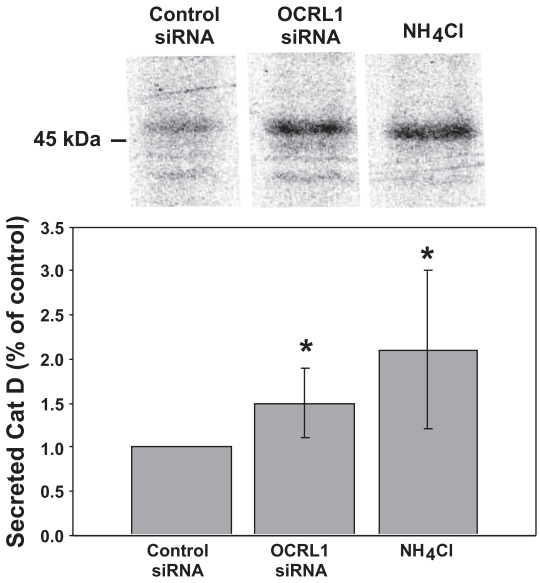

Fig. 6. Delivery of newly synthesized lysosomal hydrolases is impaired in HK-2 cells lacking OCRL1. HK-2 cells treated with control or OCRL1 siRNA were radiolabeled for 2 h and chased for 4 h. NH_4Cl (10 mM) was included in the indicated samples. Radioactive cathepsin D secreted into the media during the chase was quantitated after immunoprecipitation and SDS-PAGE and normalized relative to control. The results from 3 experiments are plotted. *$P = 0.029$ by Mann-Whitney Rank Sum test. Samples of cathepsin D immunoprecipitated from the medium in a representative experiment are shown above the graph.

enzymes are elevated in Lowe syndrome patients and with a role for OCRL1 in TGN-endosome trafficking (8, 47). Together, our data suggest that a defect in this step in membrane traffic represents the primary manifestation of cells lacking OCRL1. Below, we discuss the implications of our findings with respect to the pathogenesis of Lowe syndrome.

Phenotype of OCRL1-depleted cells. Knockdown of OCRL1 using nucleofection was efficient (80–95%) as monitored using both Western blotting and PCR. We were able to amplify endogenous message encoding INPP5B in MDCK but not in HK-2 cells. Knockdown of OCRL1 did not significantly increase cellular PIP_2 levels measured in MDCK cells but had a dramatic effect on the number of cells with detectable actin comets. Fibroblasts from Lowe syndrome patients have previously been demonstrated to have significantly elevated numbers of actin comets (1); thus, acute depletion of OCRL1 (even in cells expressing INPP5B) appears to appropriately mimic key features observed in fibroblast models for the disease. The absence of a dramatic effect on PIP_2 levels upon OCRL1 knockdown is consistent with the localization of OCRL1 to intracellular compartments and suggests that this enzyme normally does not have access to the majority of cellular PIP_2, which is localized to the plasma membrane.

OCRL1 knockdown and biosynthetic delivery. We previously found that increased cellular PIP_2 mediated by overexpression of PI5KIβ resulted in increased actin comet frequency and also enhanced biosynthetic delivery kinetics of the apical protein influenza HA (18). However, in the studies reported here, we found no effect on apical protein delivery in cells lacking OCRL1, although we did observe an increase in actin comets. PI5KIβ overexpression results in a considerably larger and statistically significant increase in cellular PIP_2 levels compared with OCRL1 knockdown, so it is possible that a threshold increase in PIP_2 is required to stimulate delivery kinetics detectably. Alternatively, the effects of PIP_2-stimulated HA delivery might not be linked directly to actin comet formation, although the selective modulation of HA delivery we observed on PI5KIβ expression, inhibition of Arp2/3 activation (18), and N-WASP knockdown (Fig. 3) would argue against this idea. Finally, actin comets stimulated by OCRL1 knockdown may emanate from sites distinct from those evoked on PI5KIβ overexpression and may not propel apically destined carriers.

Although we were unable to assess the effect of OCRL1 knockdown on megalin biosynthetic traffic, we believe it unlikely that this pathway is affected by OCRL1 depletion. Like HA, a fraction of megalin has been reported to reside in glycolipid-enriched microdomains, or lipid rafts (32), although it is not known whether the two take a similar biosynthetic route to the apical membrane. The stimulation in apical delivery we might predict in OCRL1-depleted cells (but did not observe for HA) would be expected to increase surface megalin levels and is intuitively inconsistent with a trafficking defect that would result in proteinuria. Importantly, we did not find any significant difference in the steady-state level of mini-megalin at the cell surface of control vs. OCRL1-depleted cells as assessed by Western blotting (data not shown).

OCRL1 knockdown does not disrupt megalin trafficking. OCRL1 knockdown did not affect megalin endocytosis as measured by either a biotinylated assay to detect receptor internalization or by following the fate of the radioiodinated ligand [^{125}I]Lf. The latter assay was performed using two model systems: polarized MDCK cells expressing a mini-megalin receptor and human proximal tubule cells that express endogenous megalin. Moreover, we found no effects of OCRL1 knockdown on ligand degradation when we monitored multiple rounds of uptake over a 14- to 18-h period. In contrast, we found that overexpression of PI5KIβ stimulated the rate of megalin endocytosis. Together, these results suggest the strong possibility that OCRL1 does not directly regulate megalin traffic or function along the endocytic pathway. Recent studies demonstrated that OCRL1 binds directly to clathrin heavy chain and observed a small fraction of cellular OCRL1 in association with clathrin-coated vesicles (8, 9, 16, 46). Our studies suggest that the pool of protein associated with the cell surface and very early endocytic vesicles may not have a direct role in modulating endocytosis.

On the one hand, our observations are consistent with the prediction that increased cellular PIP_2 would not alter megalin traffic in a manner that would be expected to compromise LMWP uptake. On the other hand, the lack of effect of OCRL1 depletion on megalin traffic is somewhat surprising given that effects on endocytosis of fluid phase markers and megalin ligands have been reported in two CLC-5 knockout mouse models of Dent disease (11, 40, 51). A significant fraction of patients diagnosed with Dent disease have recently been shown to have mutations in OCRL1 rather than in CLC-5 (24), suggesting that the two proteins provide critical functions along the same pathway. There is a decrease in both the overall level and the apical concentration of megalin and cubulin in the proximal tubule of mouse CLC-5 knockouts that leads to a profound decrease in the endocytosis of megalin/cubulin ligands (11, 51, 52). This effect is not universal, as no defect in

apical endocytosis or megalin function is observed in the thyroid of CLC-5 knockout mice (31, 49). It is not yet clear how loss of CLC-5 leads to the observed decrease in megalin expression and the consequent low-molecular-weight proteinuria characteristic of Dent disease patients (13, 19). Changes in megalin localization have not been observed in renal biopsies from human patients (34), although both Dent disease and Lowe syndrome patients shed significantly decreased levels of megalin into the urine (37). CLC-5 is largely localized to endocytic compartments and endosome acidification in proximal tubule cells cultured from CLC-5-deficient mice is reported to be defective (20). A small fraction of CLC-5 also localizes to the cell surface and it has also been suggested that CLC-5 plays an important role in endocytosis at the plasma membrane (25). Importantly, while there is a clear inhibition in the accumulation of ligands and fluid phase markers in proximal tubule cells from CLC-5 knockout vs. control mice (40, 52), it is not known whether the rate of endocytosis is affected. By analogy with our studies in OCRL1-depleted cells, we predict that no change would be observed in endocytosis kinetics in renal epithelial cells. Unfortunately, we could not address this directly, as we were unable, using multiple approaches, to knockdown CLC-5 in any of our renal epithelial cell lines.

OCRL1 knockdown enhances lysosomal enzyme secretion. Knockdown of OCRL1 perturbed lysosomal delivery of newly synthesized cathepsin D. This result is consistent with studies by Choudhury et al. (8) demonstrating a partial shift in the steady-state distribution of the cation-independent mannose 6-phosphate receptor from the TGN to endosomes in cells transfected with OCRL1 siRNA, as well as with the previous observation that Lowe syndrome patients have elevated serum levels of lysosomal hydrolases (47). This finding is also consistent with the primarily TGN/endosomal distribution of OCRL1.

How OCRL1 function regulates the sorting of lysosomal hydrolases is still unknown. OCRL1 interacts with numerous components of the machinery known to be involved in this process, including clathrin and several members of the rab GTPase family; however, there is no evidence that interaction with OCRL1 modulates the function of these proteins (8, 26). A more tractable possibility that has been suggested is that modulation of Golgi or endosomal PIP_2 levels by OCRL1 is important for the recruitment of adaptor proteins required for TGN to endosomal delivery (30). Alternatively, OCRL1 modulation of actin dynamics may be required for the sorting or delivery of lysosomally destined cargos.

How does loss of OCRL1 activity lead to the renal manifestations observed in Lowe syndrome patients? Our results would suggest that OCRL1 does not directly modulate the trafficking or function of megalin. Although lysosomal hydrolases bind to and can be internalized by megalin (36), it is unlikely that the slight increase in enzyme secretion we observed would significantly impede megalin binding to other ligands. Together, our results suggest that OCRL1 deficiency does not directly cause a defect in megalin trafficking or in the uptake or degradation of megalin ligands. Rather, we hypothesize that proteinuria is a downstream consequence that results from reduced levels of megalin in the renal proximal tubule of Lowe syndrome patients. We did not observe any difference in the binding or uptake of megalin ligands to HK-2 cells in which OCRL1 was acutely depleted compared with control cells and speculate that the loss of megalin results from chronic alterations in cell signaling in renal cells lacking OCRL1. To this end, it is noteworthy that both OCRL1 and CLC-5 have been suggested to associate with macromolecular complexes that include megalin at the cell surface and that could be involved in cell signaling (16, 25, 41). Additionally, megalin has been reported to undergo intramembrane proteolysis that generates a tail-containing fragment able to enter the nucleus (4). Similarly, APPL1 can translocate from endosomes to the nucleus in response to extracellular stimuli such as oxidative stress (33). Indeed, a more global response to loss of OCRL1 function is necessary to explain the other clinical abnormalities associated with Lowe syndrome. Future exploration of these possibilities will clearly be necessary to elucidate the pathway by which loss of OCRL1 function leads to renal disease in patients with Lowe syndrome.

ACKNOWLEDGMENTS

We thank M. Farquhar for constructs encoding mini-megalin, R. Nussbaum, and S. Suchy for anti-OCRL1 antibody, L. Traub for anti-Dab2 and ARH antibodies, and A. Ungewickell for advice on the OCRL1 knockdown experiments. Y. Lai provided expert technical assistance in epitope tagging and subcloning mini-megalin and other constructs. We are especially grateful to S. Guggino for advice and for providing reagents to knock down CLC-5 in renal cells.

GRANTS

This work was supported by grants from the National Institutes of Health (DK-064613), the Lowe Syndrome Association, and the Pennsylvania Department of Health to O. A. Weisz; DK-054787 (to R. P. Hughey); and by the Cellular Physiology Core of the Pittsburgh Center for Kidney Research (P30 DK079307). C. J. Guerriero was supported by T32 DK-061296 and by an American Heart Association predoctoral fellowship. C. M. Szalinski was supported in part by T32 DK-061296.

DISCLOSURES

No conflicts of interest are declared by the authors.

REFERENCES

1. **Allen PG.** Actin filament uncapping localizes to ruffling lamellae and rocketing vesicles. *Nat Cell Biol* 5: 972–979, 2003.
2. **Altschuler Y, Kinlough CL, Poland PA, Apodaca G, Weisz OA, Hughey RP.** Clathrin mediated endocytosis of MUC1 is modulated by its glycosylation state. *Mol Biol Cell* 11: 819–831, 1999.
3. **Barbieri MA, Heath CM, Peters EM, Wells A, Davis JN, Stahl PD.** Phosphatidylinositol-4-phosphate 5-kinase-1β is essential for epidermal growth factor receptor-mediated endocytosis. *J Biol Chem* 276: 47212–47216, 2001.
4. **Biemesderfer D.** Regulated intramembrane proteolysis of megalin: linking urinary protein and gene regulation in proximal tubule? *Kidney Int* 69: 1717–1721, 2006.
5. **Breitfeld PP, Casanova JE, Harris JM, Simister NE, Mostov KE.** Expression and analysis of the polymeric immunoglobulin receptor in Madin-Darby canine kidney cells using retroviral vectors. *Meth Cell Biol* 32: 329–337, 1989.
6. **Bruns JR, Ellis MA, Jeromin A, Weisz OA.** Multiple roles for phosphatidylinositol 4-kinase in biosynthetic transport in polarized MDCK cells. *J Biol Chem* 277: 2012–2018, 2001.
7. **Charnas LR, Gahl WA.** The oculocerebrorenal syndrome of Lowe. *Adv Pediatr* 38: 75–107, 1991.
8. **Choudhury R, Diao A, Zhang F, Eisenberg E, Saint-Pol A, Williams C, Konstantakopoulos A, Lucocq J, Johannes L, Rabouille C, Greene LE, Lowe M.** Lowe syndrome protein OCRL1 interacts with clathrin and regulates protein trafficking between endosomes and the *trans*-Golgi network. *Mol Biol Cell* 16: 3467–3479, 2005.

9. **Choudhury R, Noakes CJ, McKenzie E, Kox C, Lowe M.** Differential clathrin binding and subcellular localization of OCRL1 splice isoforms. *J Biol Chem* 284: 9965–9973, 2009.
10. **Christensen EI, Birn H.** Megalin and cubilin: multifunctional endocytic receptors. *Nat Rev Mol Cell Biol* 3: 256–266, 2002.
11. **Christensen EI, Devuyst O, Dom G, Nielsen R, Van der SP, Verroust P, Leruth M, Guggino WB, Courtoy PJ.** Loss of chloride channel ClC-5 impairs endocytosis by defective trafficking of megalin and cubilin in kidney proximal tubules. *Proc Natl Acad Sci USA* 100: 8472–8477, 2003.
12. **Coon BG, Mukherjee D, Hanna CB, Riese DJ, Lowe M, Aguilar RC.** Lowe syndrome patient fibroblasts display Ocrl1-specific cell migration defects that cannot be rescued by the homologous Inpp5b phosphatase. *Hum Mol Genet* In press.
13. **Devuyst O, Jouret F, Auzanneau C, Courtoy PJ.** Chloride channels and endocytosis: new insights from Dent's disease and ClC-5 knockout mice. *Nephron Physiol* 99: 69–73, 2005.
14. **Di Paolo G, De Camilli P.** Phosphoinositides in cell regulation and membrane dynamics. *Nature* 443: 651–657, 2006.
15. **Dressman MA, Olivos-Glander IM, Nussbaum RL, Suchy SF.** Ocrl1, a PtdIns(4,5)P_2 5-phosphatase, is localized to the *trans*-Golgi network of fibroblasts and epithelial cells. *J Histochem Cytochem* 48: 179–190, 2000.
16. **Erdmann KS, Mao Y, McCrea HJ, Zoncu R, Lee S, Paradise S, Modregger J, Biemesderfer D, Toomre D, De Camilli P.** A role of the Lowe syndrome protein OCRL in early steps of the endocytic pathway. *Dev Cell* 13: 377–390, 2007.
17. **Gong D, Ferrell JE Jr.** Picking a winner: new mechanistic insights into the design of effective siRNAs. *Trends Biotechnol* 22: 451–454, 2004.
18. **Guerriero CJ, Weixel KM, Bruns JR, Weisz OA.** Phosphatidylinositol 5-kinase stimulates apical biosynthetic delivery via an Arp2/3-dependent mechanism. *J Biol Chem* 281: 15376–15384, 2006.
19. **Guggino SE.** Mechanisms of disease: what can mouse models tell us about the molecular processes underlying Dent disease? *Nat Clin Pract Nephrol* 3: 449–455, 2007.
20. **Hara-Chikuma M, Wang Y, Guggino SE, Guggino WB, Verkman AS.** Impaired acidification in early endosomes of ClC-5 deficient proximal tubule. *Biochem Biophys Res Commun* 329: 941–946, 2005.
21. **Henkel JR, Apodaca G, Altschuler Y, Hardy S, Weisz OA.** Selective perturbation of apical membrane traffic by expression of influenza virus M2, an acid-activated ion channel, in polarized Madin-Darby canine kidney cells. *Mol Biol Cell* 8: 2477–2490, 1998.
22. **Henkel JR, Gibson GA, Poland PA, Ellis MA, Hughey RP, Weisz OA.** Influenza M2 proton channel activity selectively inhibits TGN release of apical membrane and secreted proteins in polarized MDCK cells. *J Cell Biol* 148: 495–504, 2000.
23. **Henkel JR, Popovich JL, Gibson GA, Watkins SC, Weisz OA.** Selective perturbation of early endosome and/or *trans*-Golgi network pH but not lysosome pH by dose-dependent expression of influenza M2 protein. *J Biol Chem* 274: 9854–9860, 1999.
24. **Hoopes RR Jr, Shrimpton AE, Knohl SJ, Hueber P, Hoppe B, Matyus J, Simckes A, Tasic V, Toenshoff B, Suchy SF, Nussbaum RL, Scheinman SJ.** Dent disease with mutations in OCRL1. *Am J Hum Genet* 76: 260–267, 2005.
25. **Hryciw DH, Ekberg J, Pollock CA, Poronnik P.** ClC-5: a chloride channel with multiple roles in renal tubular albumin uptake. *Int J Biochem Cell Biol* 38: 1036–1042, 2006.
26. **Hyvola N, Diao A, McKenzie E, Skippen A, Cockcroft S, Lowe M.** Membrane targeting and activation of the Lowe syndrome protein OCRL1 by rab GTPases. *EMBO J* 25: 3750–3761, 2006.
27. **Janne PA, Suchy SF, Bernard D, MacDonald M, Crawley J, Grinberg A, Wynshaw-Boris A, Westphal H, Nussbaum RL.** Functional overlap between murine Inpp5b and Ocrl1 may explain why deficiency of the murine ortholog for OCRL1 does not cause Lowe syndrome in mice. *J Clin Invest* 101: 2042–2053, 1998.
28. **Kempiak SJ, Yamaguchi H, Sarmiento C, Sidani M, Ghosh M, Eddy RJ, Desmarais V, Way M, Condeelis J, Segall JE.** A neural Wiskott-Aldrich Syndrome protein-mediated pathway for localized activation of actin polymerization that is regulated by cortactin. *J Biol Chem* 280: 5836–5842, 2005.
29. **Lin T, Orrison BM, Leahey AM, Suchy SF, Bernard DJ, Lewis RA, Nussbaum RL.** Spectrum of mutations in the OCRL1 gene in the Lowe oculocerebrorenal syndrome. *Am J Hum Genet* 60: 1384–1388, 1997.
30. **Lowe M.** Structure and function of the Lowe syndrome protein OCRL1. *Traffic* 6: 711–719, 2005.
31. **Maritzen T, Lisi S, Botta R, Pinchera A, Fanelli G, Viacava P, Marcocci C, Marino M.** ClC-5 does not affect megalin expression and function in the thyroid. *Thyroid* 16: 725–730, 2006.
32. **Marzolo MP, Yuseff MI, Retamal C, Donoso M, Ezquer F, Farfan P, Li Y, Bu G.** Differential distribution of low-density lipoprotein-receptor-related protein (LRP) and megalin in polarized epithelial cells is determined by their cytoplasmic domains. *Traffic* 4: 273–288, 2003.
33. **Miaczynska M, Christoforidis S, Giner A, Shevchenko A, Uttenweiler-Joseph S, Habermann B, Wilm M, Parton RG, Zerial M.** APPL proteins link Rab5 to nuclear signal transduction via an endosomal compartment. *Cell* 116: 445–456, 2004.
34. **Moulin P, Igarashi T, Van der SP, Cosyns JP, Verroust P, Thakker RV, Scheinman SJ, Courtoy PJ, Devuyst O.** Altered polarity and expression of H^+-ATPase without ultrastructural changes in kidneys of Dent's disease patients. *Kidney Int* 63: 1285–1295, 2003.
35. **Nagai M, Meerloo T, Takeda T, Farquhar MG.** The adaptor protein ARH escorts megalin to and through endosomes. *Mol Biol Cell* 14: 4984–4996, 2003.
36. **Nielsen R, Courtoy PJ, Jacobsen C, Dom G, Lima WR, Jadot M, Willnow TE, Devuyst O, Christensen EI.** Endocytosis provides a major alternative pathway for lysosomal biogenesis in kidney proximal tubular cells. *Proc Natl Acad Sci USA* 104: 5407–5412, 2007.
37. **Norden AG, Lapsley M, Igarashi T, Kelleher CL, Lee PJ, Matsuyama T, Scheinman SJ, Shiraga H, Sundin DP, Thakker RV, Unwin RJ, Verroust P, Moestrup SK.** Urinary megalin deficiency implicates abnormal tubular endocytic function in Fanconi syndrome. *J Am Soc Nephrol* 13: 125–133, 2002.
38. **Olivos-Glander IM, Janne PA, Nussbaum RL.** The oculocerebrorenal syndrome gene product is a 105-kD protein localized to the Golgi complex. *Am J Hum Genet* 57: 817–823, 1995.
39. **Padrón D, Wang YJ, Yamamoto M, Yin H, Roth MG.** Phosphatidylinositol phosphate 5-kinase Iβ recruits AP-2 to the plasma membrane and regulates rates of constitutive endocytosis. *J Cell Biol* 162: 693–701, 2003.
40. **Piwon N, Gunther W, Schwake M, Bosl MR, Jentsch TJ.** ClC-5 Cl^- channel disruption impairs endocytosis in a mouse model for Dent's disease. *Nature* 408: 369–373, 2000.
41. **Pollock CA, Poronnik P.** Albumin transport and processing by the proximal tubule: physiology and pathophysiology. *Curr Opin Nephrol Hypertens* 16: 359–364, 2007.
42. **Santo Y, Hirai H, Shima M, Yamagata M, Michigami T, Nakajima S, Ozono K.** Examination of megalin in renal tubular epithelium from patients with Dent disease. *Pediatr Nephrol* 19: 612–615, 2004.
43. **Su T, Cariappa R, Stanley K.** N-glycans are not a universal signal for apical sorting of secretory proteins. *FEBS Lett* 453: 391–394, 1999.
44. **Suchy SF, Olivos-Glander IM, Nussbaum RL.** Lowe syndrome, a deficiency of phosphatidylinositol 4,5-bisphosphate 5-phosphatase in the Golgi apparatus. *Hum Mol Genet* 4: 2245–2250, 1995.
45. **Takeda T, Yamazaki H, Farquhar MG.** Identification of an apical sorting determinant in the cytoplasmic tail of megalin. *Am J Physiol Cell Physiol* 284: C1105–C1113, 2003.
46. **Ungewickell A, Ward ME, Ungewickell E, Majerus PW.** The inositol polyphosphate 5-phosphatase Ocrl associates with endosomes that are partially coated with clathrin. *Proc Natl Acad Sci USA* 101: 13501–13506, 2004.
47. **Ungewickell AJ, Majerus PW.** Increased levels of plasma lysosomal enzymes in patients with Lowe syndrome. *Proc Natl Acad Sci USA* 96: 13342–13344, 1999.
48. **Utsch B, Bokenkamp A, Benz MR, Besbas N, Dotsch J, Franke I, Frund S, Gok F, Hoppe B, Karle S, Kuwertz-Broking E, Laube G, Neb M, Nuutinen M, Ozaltin F, Rascher W, Ring T, Tasic V, van Wijk JA, Ludwig M.** Novel OCRL1 mutations in patients with the phenotype of Dent disease. *Am J Kidney Dis* 48: 1–14, 2006.
49. **Van den Hove MF, Croizet-Berger K, Jouret F, Guggino SE, Guggino WB, Devuyst O, Courtoy PJ.** The loss of the chloride channel, ClC-5, delays apical iodide efflux and induces a euthyroid goiter in the mouse thyroid gland. *Endocrinology* 147: 1287–1296, 2006.
50. **Vicinanza M, D'Angelo G, Di Campli A, De Matteis MA.** Phosphoinositides as regulators of membrane trafficking in health and disease. *Cell Mol Life Sci* 65: 2833–2841, 2008.
51. **Wang SS, Devuyst O, Courtoy PJ, Wang XT, Wang H, Wang Y, Thakker RV, Guggino S, Guggino WB.** Mice lacking renal chloride channel, CLC-5, are a model for Dent's disease, a nephrolithiasis disorder

associated with defective receptor-mediated endocytosis. *Hum Mol Genet* 9: 2937–2945, 2000.

52. **Wang Y, Cai H, Cebotaru L, Hryciw DH, Weinman EJ, Donowitz M, Guggino SE, Guggino WB.** ClC-5: role in endocytosis in the proximal tubule. *Am J Physiol Renal Physiol* 289: F850–F862, 2005.
53. **Weixel KM, Edinger RS, Kester L, Guerriero CJ, Wang H, Fang L, Kleyman TR, Welling PA, Weisz OA, Johnson JP.** Phosphatidylinositol 4-phosphate 5-kinase reduces cell surface expression of the epithelial sodium channel (ENaC) in cultured collecting duct cells. *J Biol Chem* 282: 36534–36542, 2007.
54. **Williams C, Choudhury R, McKenzie E, Lowe M.** Targeting of the type II inositol polyphosphate 5-phosphatase INPP5B to the early secretory pathway. *J Cell Sci* 120: 3941–3951, 2007.
55. **Zhang X, Hartz PA, Philip E, Racusen LC, Majerus PW.** Cell lines from kidney proximal tubules of a patient with Lowe syndrome lack OCRL inositol polyphosphate 5-phosphatase and accumulate phosphatidylinositol 4,5-bisphosphate. *J Biol Chem* 273: 1574–1582, 1998.
56. **Zhang X, Jefferson AB, Auethavekiat V, Majerus PW.** The protein deficient in Lowe syndrome is a phosphatidylinositol-4,5-bisphosphate 5-phosphatase. *Proc Natl Acad Sci USA* 92: 4853–4856, 1995.